

Role of multiple inelastic transitions in atom transfer with the scanning tunneling microscope

R. E. Walkup, D. M. Newns, and Ph. Avouris

IBM Research Division, IBM Thomas J. Watson Research Center, Yorktown Heights, New York 10598

(Received 13 May 1992; revised manuscript received 14 October 1992)

The high current density obtainable with the scanning tunneling microscope can be used to promote multiple vibrational excitations of an adsorbate via inelastic electron tunneling. Calculations indicate that this effect plays an important role in the transfer of Xe atoms between a sample and tip by the application of current pulses. Directionality of atom transfer and applications to other systems are discussed.

The scanning tunneling microscope (STM) is becoming a unique tool for the manipulation of atoms and molecules on surfaces.^{1,2} Recent experimental progress in this area includes electric-field driven diffusion of atoms into the region under the tip,³ the precise repositioning of atoms on a surface,⁴ desorption^{5,6} and dissociation⁷ on the scale of individual molecules, and reversible transfer of atoms between the sample and the STM tip by the application of voltage pulses.^{8,9} A key feature of the STM is that very large current densities can be obtained in the tunnel junction—up to $\sim 10^{12}$ electrons s^{-1} through an area of atomic dimensions. The tunneling current can cause heating of the sample and tip,^{10,11} and it can induce vibrational excitation in an adsorbate via inelastic tunneling,^{11–15} though efforts to identify such inelastic features in STM I - V curves have not achieved much success. We argue that inelastic tunneling can have a profound effect in experiments that use the high current density of the STM to manipulate atoms and molecules. In particular, we show that for an adsorbate with a relatively long lifetime for vibrational relaxation, it is possible for the STM to induce a sequence of vibrational excitations by inelastic tunneling, and thus localize substantial energy in a bond. This energy is then available for the controlled stimulation of processes such as diffusion, desorption, dissociation, or reaction.

As a specific example of vibrational heating with the STM, we consider the recent atom-transfer experiments of Eigler, Lutz, and Rudge.⁹ In these experiments, Xe atoms were reversibly transferred between a Ni(110) surface and the STM tip by the application of voltage pulses (± 0.8 V, 64 ms). Xe atoms were transferred in the same direction as the tunneling electrons flow. For a particular tip-sample configuration, the transfer rate varied approximately as $I^{4.9}$, where I is the tunneling current. We show that such a dependence is consistent with a model in which there is stepwise excitation of the adatom-surface bond by inelastic electron tunneling.

The key features of our model are as follows: (i) a potential-energy surface for the motion of the Xe atom, including energy levels and wave functions associated with the adatom-substrate vibration and (ii) a set of rate equations (master equations) which describe vibrational transitions induced by the tunneling electrons and also by phonons. Similar approaches have been used to describe thermal desorption¹⁶ and field desorption.¹⁷ For simplicity

we consider a one-dimensional model in which the Xe atom is placed in a double-well potential. The crucial feature of this potential is the energy barrier for atom transfer from the sample to the tip. When the tip is sufficiently far from the sample, the energy barrier is the Xe-sample binding energy. As the tip is brought close to the Xe atom, the energy barrier is reduced by attractive interactions with the tip. This effect can be examined by constructing atomistic models of the sample and tip, with pair potentials to describe the Xe-sample and Xe-tip interactions. We use a pair potential with an exponential repulsive wall and “damped” multipolar attractive terms as suggested by Tang and Toennies.¹⁸ When the parameters of the pair potential are suitably chosen, a reasonable description of the interaction of Xe with Ni(110) is obtained.¹⁹ We represent the tip by a $30 \times 30 \text{ \AA}^2$ slab of atoms with the Ni(110) geometry, centered over the Xe adatom. In experiments,⁹ spontaneous transfer of Xe to the tip occurred at small tip-sample distances, implying stronger binding on the tip. Thus we increased the attractive terms in the pair potential for tip atoms. We use the resulting one-dimensional double well, in which the only relevant variable is the distance of the Xe atom from the surface. An example is shown in Fig. 1. The detailed shape of the double well is not very dependent on the parameters of the pair potential. The energy barrier for Xe

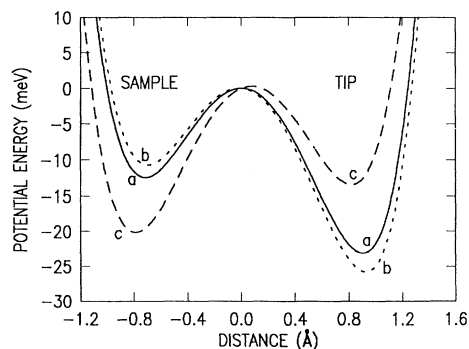


FIG. 1. The potential curve for Xe at zero bias (curve *a*) has a well on the sample (left side) and a deeper well on the tip (right side). The effect of adding a dipole potential is shown for bias voltages of -0.2 V (curve *b*) and $+0.8$ V (curve *c*) applied to the sample. Note the reversal of the asymmetry for curve *c*.

transfer from the sample to the tip depends strongly on the tip-sample separation, as shown in Fig. 2. Due to the long-range nature of the attractive forces, the tip lowers the barrier over a substantial range of tip-sample distances.

The experimentally relevant range of energy barriers can be estimated as follows. Spontaneous transfer of Xe to the tip occurred at small tip-sample separations.⁹ From the measured junction impedances one can conclude that current-driven transfer rates were measured at ≈ 0.1 Å outward displacement of the tip from the point of spontaneous transfer. If we regard spontaneous transfer as thermally activated at the ambient temperature of 4 K, then a spontaneous transfer rate of ~ 1 s⁻¹ would correspond to an energy barrier of ~ 9 meV.²⁰ From our pair-potential calculations, an outward tip displacement of ≈ 0.1 Å would then correspond to barrier heights of ~ 14 meV—see Fig. 2. Thus we have carried out calculations for barriers in the 10–20-meV range.

The kinetics of atom transfer are described by rate equations. First, the quantum mechanically exact vibrational energy levels and wave functions are obtained for Xe in a double-well potential.²¹ For the double well of Fig. 1 (curve *a*) there are six states below the barrier localized on the sample, and ten states localized on the tip, as illustrated in Fig. 3. Rates are used to describe transitions between the vibrational states due to interactions with tunneling electrons and phonons. Two mechanisms for inelastic tunneling are important: (i) tunneling via the Xe “6s” resonance and (ii) dipole excitation. In resonant tunneling,¹⁵ the electron can be regarded as temporarily hopping onto the Xe atom, forming a transient negative ion. During the resonance lifetime the Xe atom experiences a force which results in a small probability for vibrational excitation. From the model of Persson and Baratoff,¹⁵ we estimate that the ratio of inelastic to elastic tunneling conductance (for the $v=0$ to 1 vibration) is $\sim 3 \times 10^{-4}$.²² The tunneling electrons also interact with

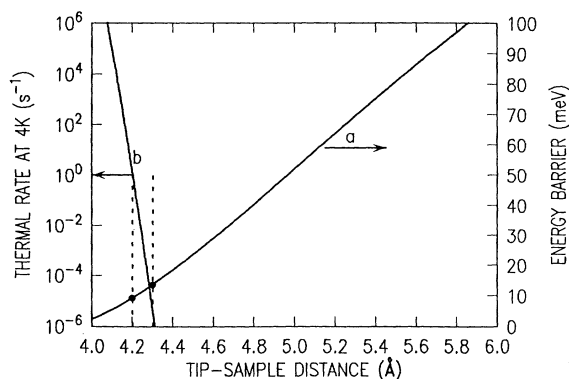


FIG. 2. The calculated energy barrier for transfer of Xe from the sample to the tip is shown (curve *a*) as a function of tip-sample distance. The thermally activated transfer rate at 4 K (curve *b*) is also shown. The thermal rate is ~ 1 s⁻¹ at a tip-sample distance of ≈ 4.2 Å, where the energy barrier is ≈ 9 meV. Increasing the tip-sample distance by 0.1 Å results in a barrier of ≈ 14 meV.

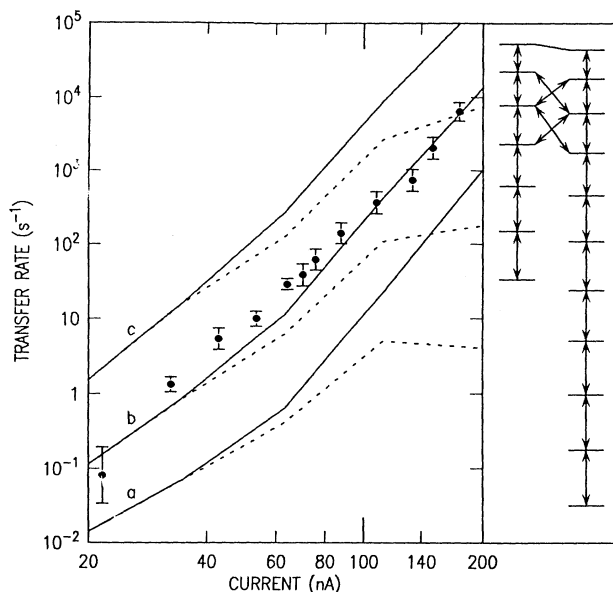


FIG. 3. The left panel shows the rate of current-driven transfer of Xe from the sample to the tip for negative bias (solid lines) and positive bias (dotted lines) applied to the sample, with inelastic tunneling fractions of 3×10^{-4} (curve *a*), 6×10^{-4} (curve *b*), and 1.2×10^{-3} (curve *c*). Experimental data of Eigler, Lutz, and Rudge (Ref. 9) are shown for comparison (dots with error bars). The right panel shows a typical energy-level scheme used in the rate equations. Transitions occur stepwise on the vibrational ladder, and atomic tunneling is included for levels near the top of the barrier. States above the barrier are replaced by a single effective level.

the transition dipole moment of the adatom-surface vibration. The dipole mechanism¹¹ yields an inelastic tunneling fraction of $\approx (\mu_{01}/ea_0)^2$, where μ_{01} is the transition dipole moment and a_0 is the bohr radius. From the dipole moment function of Lang,²³ we estimate an inelastic tunneling ratio of $\sim 2 \times 10^{-4}$ for the dipole mechanism. This is comparable to the estimate for the resonance mechanism. In the resonance mechanism, transitions other than $\Delta v = \pm 1$ are negligible owing to the short resonance lifetime.¹⁵ Also, the rate for $n-1 \rightarrow n$ is larger than the $0 \rightarrow 1$ rate by a multiplicative factor of n . This is a consequence of a linear expansion and the result that for a harmonic oscillator $|\langle n-1|x|n \rangle|^2 \propto n$. The same scaling relation approximately holds for dipole excitation owing to a similar linear expansion. Thus all of the relevant inelastic tunneling rates are proportional to the $v=0$ to 1 rate, and the atom moves on a vibrational ladder by taking steps of $\Delta v = \pm 1$, as illustrated in Fig. 3.²⁴

Relaxation of the Xe-surface vibration occurs by energy transfer to metal phonons. We have estimated the relaxation rates as follows: (i) classical-trajectory calculations for Xe interacting with a large metal cluster,²⁵ (ii) the distorted-wave, Born approximation,²⁵ and (iii) a simple model²⁶ in which the metal is treated as an elastic continuum driven by the vibrating atom. These three approaches yield closely similar results (within a factor of

2), and indicate that the continuum model²⁶ is adequate. This model yields an ≈ 25 -ps lifetime for the $v = 1$ level in our potential well. The higher vibrational levels decay by transitions with $\Delta v = 1$ and 2, with rates that reflect the anharmonic character of the potential.²⁷ Rates for excitation by metal phonons are related to the downward relaxation rates by detailed balance at 4 K, thus assuring equilibrium in the absence of current flow. Tunneling of the Xe atom near the top of the barrier is included in the rate equations. A more detailed description will be presented elsewhere.²⁵

An estimate of current-driven vibrational excitation can now be obtained. In steady state, there is a balance between excitation and relaxation, which for small currents yields a population in $v = 1$ of $n_1 \approx n_0(I/e)f_{\text{in}}\tau$, where n_0 is the ground-state population, I is the current, f_{in} is the inelastic tunneling fraction, and τ is the lifetime of the $v = 1$ level. For a harmonic vibration, the steady-state population of higher levels falls off as successive powers of $[(I/e)f_{\text{in}}\tau]$.²⁸ With $\tau = 25$ ps, $I = 200$ nA, and $f_{\text{in}} = 5 \times 10^{-4}$, one has a population ratio $n_1/n_0 \approx 1.5 \times 10^{-2}$, which for a level spacing of $\hbar\omega \approx 2.5$ meV corresponds to an effective vibrational temperature of ≈ 7 K. Thus inelastic tunneling can substantially heat the vibrational mode above the ambient temperature (4 K).

We next examine the directionality of atom transfer. Several mechanisms including multipolar interactions and the electron wind force²⁹ have been considered. Estimates for Xe indicate that the adsorption-induced dipole is the dominant effect, as suggested by Cerda *et al.*³⁰ Xe adsorption lowers the work function,³¹ indicating a dipole of ~ 0.3 D.³² According to local-density calculations,^{23,33,34} the dipole moment depends strongly on the Xe-surface distance. Since the sample and tip surfaces oppose each other, the dipole takes on opposite signs for adsorption on the sample and tip. In the presence of an applied field this gives rise to a directional force on the Xe atom, $F = (\partial\mu/\partial x)V_{\text{bias}}/w$, where $\mu(x)$ is the dipole moment, V_{bias} is the voltage applied to the sample, and w is the distance between image planes on the sample and tip. We approximate $\mu(x)$ for Xe in a bimetallic junction by a sum of dipoles for the two opposing surfaces, $\mu(x) = \mu_0/[\alpha + \beta(x/L)^4] - \mu_0/[\alpha + \beta(w - x/L)^4]$, where $\mu_0 = 0.3$ D, $\alpha = 0.3$, $\beta = 0.7$, x is the Xe distance from a reference plane on the sample, and we take $w = 4.4$ Å and $L = 1.56$ Å. These parameters reproduce the calculated $\mu(x)$ for a single surface.²³ The effect of the dipole term on the double well is shown in Fig. 1 for bias voltages of 0 (curve *a*), -0.2 V (curve *b*), and $+0.8$ V (curve *c*). The sign of the dipole effect favors Xe adsorption on the positively biased electrode. Atom transfer at low bias voltages ($|V| < 0.1$ V) is not very dependent on the dipole term. However, this term gives rise to reversible transfer at higher voltages, as evidenced by the reversal in the asymmetry of the double well at $+0.8$ V (curve *c*).

The rate equations predict exponential decay of the probability to find the Xe atom on the sample side of the barrier, as seen in experiment.⁹ The transfer rate from sample to tip is defined by $R_{S \rightarrow T} = -\sum_n \dot{c}_n P_S(n) / \sum_n c_n P_S(n)$, where c_n is the probability of finding the atom in the n th vibrational state and $P_S(n)$

the net probability for the n th state to be on the sample side of the barrier. $R_{S \rightarrow T}$ is an ensemble-averaged rate, which is directly related to an average obtained by repeated measurements on a single atom, as done by Eigler, Lutz, and Rudge.⁹ The calculated transfer rate is shown in Fig. 3 for a sequence of assumed $0 \rightarrow 1$ inelastic tunneling fractions and for positive as well as negative bias voltages. The calculations use the double-well potential of Fig. 1. Reasonable agreement with experiment is obtained for an inelastic tunneling fraction of 6×10^{-4} and a negative bias applied to the sample (solid curve *b*). The calculated rate differs from a pure power law because there are several competing paths for barrier crossing (thermal excitation, current-driven excitation, and atomic tunneling), and also because the barrier height varies with the applied electric field. For small currents (< 50 nA) the transfer rate is predicted to be independent of the direction of current flow. In the low current regime, inelastic tunneling simply heats the atom—the fields and currents are too small to provide substantial directionality. For higher fields atom transfer becomes highly directional due to the dipole term in the potential. For $+0.8$ V applied to the sample (see Fig. 1, curve *c*), the calculated transfer rate from sample to tip is smaller than the tip-to-sample rate by a factor of $\sim 4 \times 10^{-4}$. From the magnitude of the rates, a 64-ms pulse would transfer a Xe atom on the tip back to the sample with a probability near unity (≈ 0.9996). Similarly, a -0.8 -V, 64-ms pulse applied to the sample would transfer Xe to the tip. Thus our results are consistent with reversible switching of Xe at ± 0.8 V.⁹

Si atoms have also been reversibly transferred with a STM by voltage pulses.³⁵ As for Xe, the proximity of the tip substantially lowers the energy barrier for atom transfer, but for Si, chemical interactions are relevant instead of van der Waals forces. Si atoms were transferred to the negatively biased electrode, which is opposite to the direction of Xe transfer. Directionality for Si results from the substantial changes in chemisorption that occur in the presence of very strong electric fields, as discussed by Lang.³⁶ The dipole force³⁰ sketched above for Xe is too weak to substantially affect Si. Also, in contrast to Xe, inelastic tunneling is not expected to significantly heat the Si-substrate bond because of strong coupling of this vibration to phonons. However, for other systems, such as H chemisorbed on Si, vibrational relaxation is inefficient, and local heating by the tunneling current can again play an important role.

Current-driven atom transfer is closely related to electromigration.²⁹ Recently, Ralls, Ralph, and Buhrman³⁷ demonstrated local heating of a defect above the lattice temperature, and Eigler and co-workers have suggested that Xe transfer occurs by thermally assisted electromigration.^{1,9} Our model is similar in spirit, but with different sources of heating and directionality than are usually discussed in the context of electromigration.²⁹ Since current flow is directional, energy transfer by inelastic tunneling should be accompanied by a net transfer of momentum to the Xe atom. In a simple picture, the average momentum change per electron, Δp , would be related to the average energy transfer, ΔE , by

$\Delta E \sim (\Delta p)^2/2M$, where M is the Xe mass. Momentum transfer results in an "electron wind" force $F_w \simeq (I/e)\Delta p$. For our model tunnel junction this wind force is estimated to be a factor of ~ 10 smaller than the dipole force, and was thus neglected. However, for low impedance tunnel junctions the electron wind may contribute to directional atom transfer.

In conclusion we have shown that the STM current can produce multiple vibrational excitation of an adsorbate via inelastic electron tunneling. This opens new possibilities for atomic and molecular manipulation with the STM, and suggests new experimental approaches for identifying inelastic tunneling processes. Significant vibrational heating can be achieved with the STM for sys-

tems with long vibrational lifetimes, such as physisorbed Xe or chemisorbed H atoms. Measurements by Eigler, Lutz, and Rudge⁹ of current-driven transfer of Xe atoms are consistent with an inelastic tunneling fraction of $\sim 6 \times 10^{-4}$, which is comparable to theoretical estimates for the resonance¹⁵ and dipolar¹¹ mechanisms. Similar results were recently described by S. Gao, M. Persson, and B. I. Lundqvist, *Solid State Commun.* **84**, 271 (1992).

ACKNOWLEDGMENTS

We thank D. M. Eigler, B. N. J. Persson, and N. D. Lang for helpful discussions, and P. Echenique for providing Ref. 30 prior to publication.

¹J. A. Strosio and D. M. Eigler, *Science* **254**, 1319 (1991).

²C. F. Quate, in *Proceedings of the NATO Science Forum '90*, edited by L. Easki (Plenum, New York, in press).

³L. J. Whitman, J. A. Strosio, R. A. Dragoset, and R. J. Celotta *Science* **251**, 1206 (1991).

⁴D. M. Eigler and E. K. Schweizer, *Nature* **344**, 524 (1990).

⁵R. S. Becker, G. S. Higashi, Y. J. Chabal, and A. J. Becker, *Phys. Rev. Lett.* **65**, 1917 (1990).

⁶I.-W. Lyo and Ph. Avouris, *J. Chem. Phys.* **93**, 4479 (1990).

⁷G. Dujardin, R. E. Walkup, and Ph. Avouris, *Science* **255**, 1232 (1992).

⁸I.-W. Lyo and Ph. Avouris, *Science* **253**, 173 (1991).

⁹D. M. Eigler, C. P. Lutz, and W. E. Rudge, *Nature* **352**, 600 (1991).

¹⁰F. Flores, P. M. Echenique, and R. H. Ritchie, *Phys. Rev. B* **34**, 2899 (1986).

¹¹B. N. J. Persson and J. E. Demuth, *Solid State Commun.* **57**, 769 (1986).

¹²R. C. Jaklevic and J. Lambe, *Phys. Rev. Lett.* **17**, 1139 (1966).

¹³D. J. Scalapino and S. M. Marcus, *Phys. Rev. Lett.* **18**, 459 (1967).

¹⁴P. K. Hansma, in *Vibrational Spectroscopy of Molecules on Surfaces*, edited by J. T. Yates, Jr. and T. Madey (Plenum, New York, 1987), p. 135.

¹⁵B. N. J. Persson and A. Baratoff, *Phys. Rev. Lett.* **59**, 339 (1987).

¹⁶H. J. Kreuzer and Z. W. Gortel, *Physisorption Kinetics* (Springer-Verlag, Berlin, 1986).

¹⁷M. Tsukada and Z. W. Gortel, *Phys. Rev. B* **38**, 3892 (1988).

¹⁸K. T. Tang and J. P. Toennies, *J. Chem. Phys.* **80**, 3726 (1984).

¹⁹The pair potential has the form $U_{\text{pair}}(R) = U_0 e^{-b(R-R_0)} - f_6 C_6 R^{-6} - f_8 C_8 R^{-8} - f_{10} C_{10} R^{-10}$, where the f_n 's are damping functions (Ref. 18), and $U_0 = 1.0$ eV, $b = 2.60 \text{ \AA}^{-1}$, $R_0 = 2.40 \text{ \AA}$, $C_6 = 95 \text{ eV \AA}^6$, $C_8 = 950 \text{ eV \AA}^8$, and $C_{10} = 9500 \text{ eV \AA}^{10}$.

²⁰Thermally activated transfer proceeds with a rate $\sim \nu e^{-\Delta E/kT}$,

with $\nu \sim 6 \times 10^{11} \text{ s}^{-1}$ (comparable to the Xe oscillation frequency).

²¹M. D. Feit, J. A. Fleck, Jr., and A. Steiger, *J. Comput. Phys.* **47**, 412 (1982).

²²We take the "6s" resonance as $\simeq 4$ eV above the Fermi level, with a width of ~ 1 eV; see K. Wandelt, W. Jacob, N. Memmel, and V. Dose, *Phys. Rev. Lett.* **57**, 1643 (1986); D. M. Eigler, P. S. Weiss, E. K. Schweizer, and N. D. Lang, *ibid.* **66**, 1189 (1991).

²³N. D. Lang, *Phys. Rev. Lett.* **46**, 842 (1981).

²⁴Calculations for the dipole mechanism show that overtones do not affect the transfer rate at currents $\gtrsim 100$ nA, but may contribute at low currents, thus softening the current dependence.

²⁵R. E. Walkup, D. M. Newns, and Ph. Avouris (unpublished).

²⁶B. N. J. Persson and R. Ryberg, *Phys. Rev. B* **32**, 3586 (1985).

²⁷The relaxation rate is taken as that for a harmonic oscillator with the correct transition frequency and energy above the zero point.

²⁸N. G. van Kampen, *Stochastic Processes in Physics and Chemistry* (North-Holland, Amsterdam, 1981).

²⁹See, for example, A. H. Verbruggen, *IBM J. Res. Dev.* **32**, 93 (1988).

³⁰J. R. Cerda, F. Flores, P. L. de Andres, and P. M. Echenique (unpublished).

³¹See, for example, K. Wandelt and J. E. Hulse, *J. Chem. Phys.* **80**, 1340 (1984).

³²C. P. Flynn and Y. C. Chen, *Phys. Rev. Lett.* **46**, 447 (1981).

³³J. E. Müller, *Phys. Rev. Lett.* **65**, 3021 (1990).

³⁴I. V. Udatchin, A. L. Ivanovsky, and V. A. Gubanov, *Surf. Sci.* **225**, 184 (1990).

³⁵I.-W. Lyo and Ph. Avouris, *Science* **253**, 173 (1991).

³⁶N. D. Lang, *Phys. Rev. B* **45**, 13 599 (1992).

³⁷K. S. Ralls, D. C. Ralph, and R. A. Buhrman, *Phys. Rev. B* **40**, 11 561 (1989).